One-Dimensional Chainlike Arrays of Fe 3 O 4 Hollow Nanospheres Synthesized by Aging Iron Nanoparticles in Aqueous Solution

ARTICLE *in* THE JOURNAL OF PHYSICAL CHEMISTRY C · JULY 2009

Impact Factor: 4.77 · DOI: 10.1021/jp810662j

6 AUTHORS, INCLUDING:

Chinping Chen
Peking University
96 PUBLICATIONS **1,662** CITATIONS

One-Dimensional Chainlike Arrays of Fe_3O_4 Hollow Nanospheres Synthesized by Aging Iron Nanoparticles in Aqueous Solution

Jing Huang,[†] Weimeng Chen,[§] Wei Zhao,[†] Yaoqi Li,[†] Xingguo Li,*[,†,‡] and Chinping Chen[§]

Beijing National Laboratory for Molecular Sciences (BNLMS) (The State Key Laboratory of Rare Earth Materials Chemistry and Applications), College of Chemistry and Molecular Engineering, College of Engineering, and Department of Physics, Peking University, Beijing 100871, P.R. China

Received: December 3, 2008; Revised Manuscript Received: May 23, 2009

One-dimensional (1D) chainlike arrays of hollow magnetic Fe_3O_4 spheres have been prepared by simply aging magnetically preassembled Fe nanoparticles in aqueous solution at room temperature. The diameter of the 1D nanomaterials is about 100−200 nm, and the length is up to 1−3 μm, observed by scanning electron microscopy (SEM) and transmission electron microscopy (TEM). The structure and magnetic properties of the Fe_3O_4 hollow chains were characterized by X-ray powder diffraction (XRD) and via a superconducting quantum interference device (SQUID) magnetometer. Mechanism investigations on the time dependent process reveal these hollow nanostructures were formed based on the nanoscale Kirkendall effect. Besides the aqueous microenvironment, the partial pressure of oxygen is of great importance in the formation of 1D chainlike Fe_3O_4 hollow nanostructures.

Introduction

Nano- and microscale hollow spheres have received much attention in recent years because of their intriguing properties and potential applications in catalysis, optical devices, drug delivery, controlled release, chemical sensors, and biotechnology.[1−6] Within these materials, magnetic hollow spheres compose an important class. Much effort has been devoted to the synthesis of diverse magnetic hollow spheres such as Ni, Co, CoPt, NiPt, FeCo, and ferrites.[7−18] Above all, Fe_3O_4 nanoparticles with hollow structures have attracted a great deal of interest because of their challenging properties, such as low density, large specific area, drug delivery, and controlled release.[13−18]

In addition, one-dimensional (1D) chains of magnetic nanoparticles have become increasingly important both fundamentally and technologically, as their assembly behaviors efficiently affect the intrinsic properties (electronic, optical, mechanical, and magnetic properties, etc.) and subsequent applications. Organized 1D assemblies of magnetic nanoparticles have been directly observed in solution using cryogenic electron microscopy.[19] There have also been some reports on synthesizing 1D assemblies of magnetic nanoparticle using polymer coating or molecular linker to strengthen the linked chains physically or chemically.[20−22] Up to now, only a few examples of fabricating 1D magnetic hollow sphere chains have been reported, such as Co,[8] Fe,[23] Ni,[24] and PtCo alloy.[10] Besides the gas bubble inducement, the nanoscale Kirkendall effect has emerged as a novel approach for the fabrication of hollow nanostructures. Alivisatos and co-workers first proposed "the nanoscale Kirkendall effect" to describe the synthesis of hollow CoS (CoO) nanoparticles by sulfidation (oxidation) of Co nanoparticles.[1] Nanoscale voids were formed because the outward diffusion of cobalt was dominant compared with the inward diffusion of sulfur/oxygen. Isolated hollow magnetic iron oxide nanoparticles have also been prepared by oxidation of Fe nanoparticles in organic solvent (e.g., 1-octadecene) at the temperature above 473 K via the nanoscale Kirkendall effect.[13,25] To the best of our knowledge, 1D chains of Fe_3O_4 hollow nanosphere building blocks synthesized in aqueous solution at room temperature have not yet been reported.

In this work, we carried out the synthesis of 1D chainlike hollow magnetic Fe_3O_4 spheres through *in situ* slow oxidation by simply aging magnetically preassembled Fe nanoparticles in aqueous solution. The procedure is performed at room temperature and without the requirement of cross-link reagents, which is environmentally benign. This synthetic strategy can be readily extended to produce other 1D iron based hollow nanostructures. The possible formation mechanism of these hollow nanostructures is proposed based on the results, and the magnetic properties are studied. This unique 1D chainlike hollow Fe_3O_4 structure is expected to be used in magnetic, catalytic, and biomedical applications.

Experimental Section

In a typical 1D hollow Fe_3O_4 nanospheres synthesis, ferrous sulfate heptahydrate ($FeSO_4 \cdot 7H_2O$, 0.15 mmol) and cetyltrimethylammonium bromide (CTAB, 0.5 mmol) were first dissolved in 50 mL of deionized water in a 150 mL round-bottomed flask. This procedure was with the assistance of ultrasonication under an argon atmosphere. A freshly prepared solution of sodium borohydride ($NaBH_4$, 0.4 M, 2 mL) was then added dropwise under magnetic stirring. Stirred for about 3 min, the transparent solution abruptly turned black, indicating the production of iron nanoparticles. After 30 min, the solution was exposed to the atmosphere composed of argon and air (95:5). After 24 h, the brownish precipitate was collected by centrifugation, washed with deionized water and absolute ethanol three times to remove surfactant residues, and then dried under an argon atmosphere at room temperature. Brownish 1D chainlike hollow Fe_3O_4 nanospheres were obtained.

* To whom correspondence should be addressed. E-mail: xgli@pku.edu.cn.
[†] Beijing National Laboratory for Molecular Sciences (BNLMS) (The State Key Laboratory of Rare Earth Materials Chemistry and Applications), College of Chemistry and Molecular Engineering.
[§] Department of Physics.
[‡] College of Engineering.

10.1021/jp810662j CCC: $40.75
Published on Web 06/22/2009

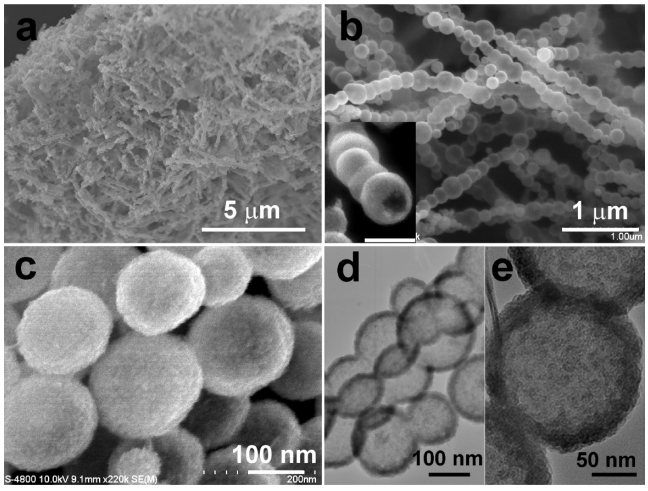

Figure 1. Morphology of the as-obtained Fe_3O_4 hollow nanospheres: (a,b) Low-magnification and (c) high-magnification SEM images; the inset of (b) shows a broken hollow sphere. The scale bar is 200 nm. (d) Low-magnification and (e) high-magnification TEM images.

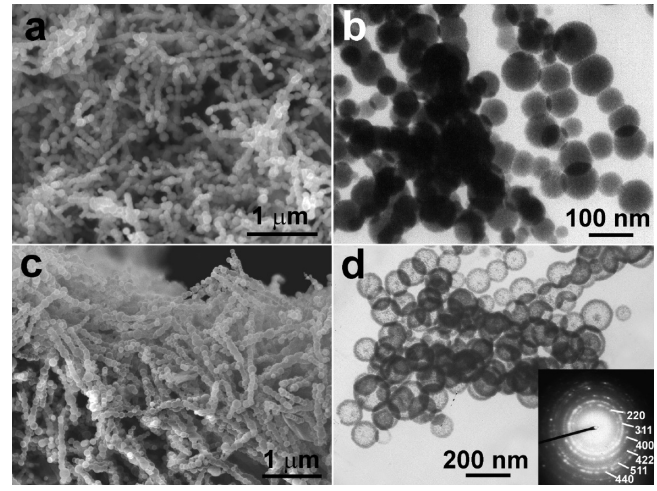

Figure 2. (a,b) SEM and TEM image of the freshly prepared Fe nanoparticles before oxidation and (c,d) SEM and TEM image of the as-obtained 1D chains of Fe_3O_4 hollow nanospheres. The inset of (d) shows an SAED pattern of the hollow Fe_3O_4 nanomaterials.

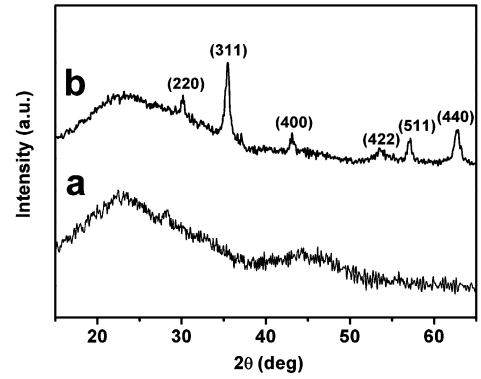

Figure 3. Powder XRD patterns of (a) the freshly prepared Fe nanoparticles before oxidation and (b) the as-obtained 1D chains of Fe_3O_4 hollow nanospheres.

The morphology and size distribution of the samples were observed by scanning electron microscopy (SEM, Hitachi S4800, 10 kV), transmission electron microscopy (TEM, JEOL JEM-200CX, 160 kV), and high-resolution transmission electron microscopy (HRTEM, Philips CM20, 200 kV). The structural analysis of the samples was carried out by X-ray diffraction (XRD, Rigaku D/max-2000 diffractometer, Cu Kα) and selected area electron diffraction (SEAD). Magnetic measurements were performed using a superconducting quantum interference device (SQUID) magnetometer (Quantum Design MPMS). Details are given as Supporting Information.

Results and Discussion

SEM and TEM were used to characterize the morphology and structure of the as-obtained samples. A typical SEM image presented in Figure 1a reveals that the as-obtained samples are fairly uniform in 1D chainlike shape with lengths of up to 1−3 μm. Close examination shows that these 1D nanomaterials are composed of interconnected nanospheres (Figure 1b, c). The average diameter of the nanospheres is in the range of 100−200 nm, which is confirmed by the TEM images shown in Figure 1d, e. The TEM images of these nanospheres are consistent with hollow structures. The edges of the spheres are much darker than the center regions, indicating that there is a void space in the center of each sphere. From a broken nanosphere (inset, Figure 1b), it can be observed that the shell thickness of these hollow spheres is about 15−20 nm, in accordance with the TEM images. The high-magnification SEM image shows that the large spherical particles have a rough appearance and are composed of many small nanoparticles (Figure 1c), which can also be observed from the TEM image (Figure 1e).

In this work, the preassembled Fe nanospheres are responsible for the formation of 1D hollow Fe_3O_4 nanosphere arrays. Similar synthetic routes have been demonstrated while synthesizing 1D hollow cobalt-based nanomaterials through magnetically presembled Co nanoparticles, for example, noble metal,[26] cobalt chalcogenide,[27,28] and cobalt platinum alloy.[10] During the preparation process of 1D hollow Fe_3O_4 chains, magnetic stirring was employed, which could induce the freshly synthesized Fe nanoparticles to form 1D chainlike structures by dipolar interactions. The chainlike arrays failed to form when the applied magnetic field was not sufficient (see Supporting Information Figure S1). We observed that the products before the oxidation were chainlike solid iron nanoparticle arrays with diameters of 80−100 nm and lengths of up to submicrometers (Figure 2a, b). Compared with the length of Fe nanoparticle arrays, the arrays of Fe_3O_4 hollow spheres are much longer, increasing up to 1−3 μm (Figure 2c, d). This may be attributed to the stronger dipolar interactions during the long aging time. The corresponding SAED pattern (inset of Figure 2d) suggests the Fe_3O_4 spheres are polycrystalline. The diffraction rings display clearly regular diffraction rings corresponding to the (220), (311), (400), (422), (511), and (440) planes of Fe_3O_4, which agree well with the XRD result. No obvious diffraction peaks are present in the XRD pattern of the freshly prepared Fe nanoparticles, indicating that the Fe particles are amorphous (Figure 3a). After controlled oxidation at room temperature for 24 h, the XRD pattern shows a poorly crystallized face-centered cubic structure (Figure 3b). The characteristic peaks of (220), (311), (400), (422), (511), and (440) corresponding to the Fe_3O_4 phase with the face-centered cubic structure (JCPDS File No. 77-1545) can be identified. The average crystallite size, calculated from the Scherrer equation, is approximately 20 nm.

Time dependent study on the product morphologies was carried out to study void evolution in the amorphous Fe nanoparticles during the controlled oxidation process. Figure 4 shows a series of TEM images of the nanoparticles at different reaction times, which indicates the probable formation mech-

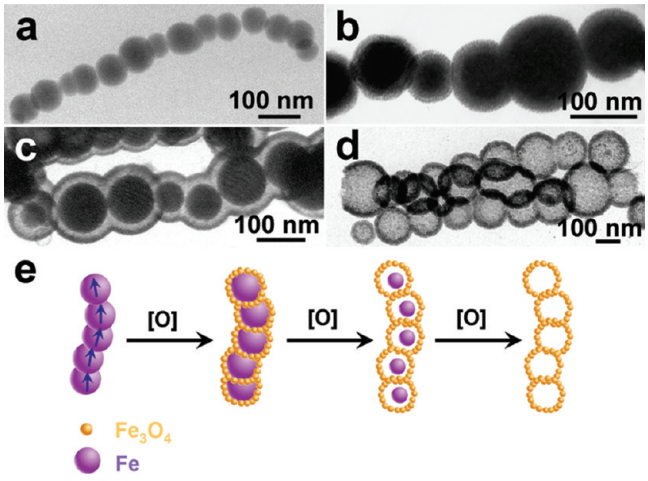

Figure 4. TEM images of (a) iron nanoparticles and the products at different stages during the formation of hollow Fe_3O_4 spheres: (b) 3 h, (c) 12 h, and (d) 24 h. (e) Schematic illustration of the formation of hollow Fe_3O_4 nanospheres.

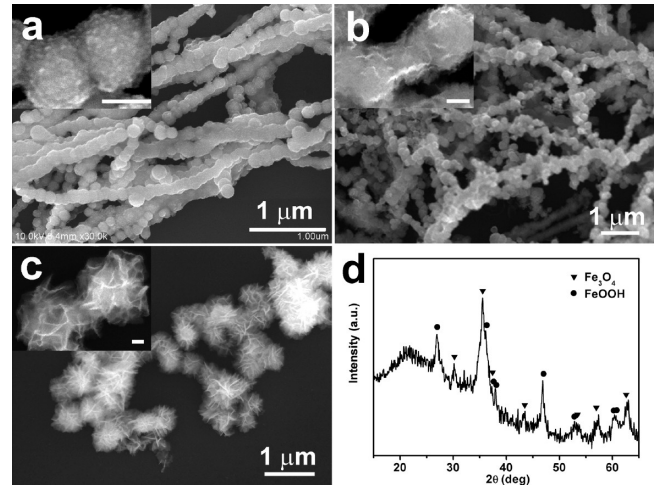

Figure 5. (a−c) SEM images of nanoparticles obtained at different stages during direct oxidation of Fe nanoparticles in air atmosphere: (a) 3 h, (b) 12 h, and (c) 24 h. The scale bar of the insets is 100 nm. (d) Powder XRD patterns of the flowerlike particles obtained from direct oxidation in air atmosphere.

anism of the 1D hollow spheres. First, solid Fe nanospheres around 80−100 nm in diameter were obtained after $NaBH_4$ was added to the Fe^{2+} solution (Figure 4a). These freshly prepared Fe nanoparticles were assembled into a 1D chainlike structure because of the dipolar interactions between each other. These solid iron sphere chains were then slowly oxidized *in situ* in aqueous solution at room temperature. At the first stage (∼3 h), an incompact layer of iron oxide generated on the surface of freshly prepared Fe nanospheres without visible gaps (Figure 4b). After 12 h oxidation, the nanospheres showed well-defined core, hollow, and shell regions (Figure 4c), as similarly observed while oxidizing Co or Fe nanoparticles in organic solvent.[1,13,25] This might be attributed to the aggregation of the smaller particles composing iron oxide shells and subsequent formation of compact shells of mixed-valence Fe(II)−Fe(III) phases. This new component shell is passive and stable in aqueous solution.[29] The formation of a relatively compact shell leads to the void between the iron core and the iron oxide shell. After 24 h oxidation, the iron core was consumed due to the outward mass transport to form the oxide shell, resulting in spherical void space in the center of the nanoparticles. 1D chainlike Fe_3O_4 hollow spheres were obtained (Figure 4d). The overall reaction can be described by the following equations:

$$Fe^{2+} + 2BH_4^- + 6H_2O = Fe^0\downarrow + 2H_2BO_3^- + 2H^+ + 7H_2\uparrow \quad (1)$$

$$3Fe + 2O_2 + nH_2O = Fe_3O_4\cdot nH_2O \quad (2)$$

$$Fe_3O_4\cdot nH_2O = nH_2O + Fe_3O_4 \quad (3)$$

The formation of 1D Fe_3O_4 hollow spheres is supposed to be directed by the nanoscale Kirkendall effect as illustrated in Figure 4e. A similar process has been demonstrated by Cabot et al.[25] while observing the reactions of Fe nanoparticles with gas phase oxygen and Peng and Sun[13] with oxygen-transfer reagent trimethylamine N-oxide (Me_3NO). As the metal component diffuses faster in a diffusion couple of metal and oxygen,[30] Fe_3O_4 hollow structures are formed while the outward diffusion rate of Fe is much larger than the inward diffusion rate of oxygen. Extensive research work has been carried out to understand the nature of this oxidation process. Interestingly, the hollow spheres we obtained are much larger than the accepted critical size of ∼8 nm for which Fe nanoparticles could completely convert into hollow iron oxide at temperature lower than 523 K.[31,25] Larger particles are supposed to be oxidized into core−shell−void structures while oxidized at lower temperature, because the iron outward transport will be reduced by the coalescence of vacancies at the metal/oxide interface. The present results might be attributed to the relatively slower diffusion of oxygen as the supply of oxygen was insufficient due to the small amount introduced and subsequently dissolved in water. Consequently, the reaction front was restricted at the oxygen/oxide interface. On the other hand, estimation has been made with the Caberra−Mott model that, at room temperature, it takes about 600 years for 4 nm thick oxide layers in iron films in a dry environment.[31,32] In this work, the aqueous environment is believed to provide unique opportunity for faster growth of oxide shells at room temperature. The attachment of oxygen onto the surface and the electron tunnels through the thin oxide layer differ from these in organic solvent or without solvent. Cabot et al. have found that the same Fe nanoparticles oxidized into hollow structure without solvent while leaving fragmented shells in the present of a solvent.[25]

In general, the oxidation behavior of Fe nanoparticles would be affected by factors such as the structural nature of Fe, concentration of oxygen reagents, microenvironment, temperature, and time.[31,25] In this work, since the Fe nanoparticles are oxidized by the oxygen dissolved in aqueous solution, the oxygen partial pressure above the solution seems to be a crucial factor. To illustrate this point, the control experiment was conducted by aging the aqueous solution directly in air with other fixed conditions. As time went on, the Fe nanoparticles in aqueous solution directly exposed to air became rough and incompact, and eventually oxidized to form spherical flowerlike particles composed of nanosheets (Figure 5a−c). No 1D hollow structures were observed probably because the partial pressure of oxygen affected the amount of dissolved oxygen in aqueous solution and thus destroyed the unbalanced interfacial diffusion of oxygen and Fe atoms during the oxidation process. XRD patterns indicate the flowerlike nanoparticles are composed of Fe_3O_4 and FeOOH (Figure 5d). Similar investigations have been observed in the synthesis of Fe_3O_4 nanosheets on a pure Fe

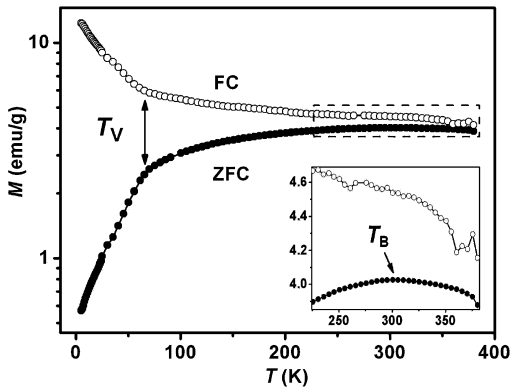

Figure 6. FC and ZFC $M(T)$ measurements of the chainlike Fe_3O_4 hollow nanospheres in log Y scale. Both of the curves were recorded in the applied field, $H_{app} = 90$ Oe, in the warming process from $T =$ 5 to 380 K. Before the warming for data collection, the field applied during the process of sample-cooling is 10 kOe for the FC measurement and 0 Oe for the ZFC measurement. The inset shows an enlarged view of the $M(T)$ curves in the high-temperature region, marked by the dashed box.

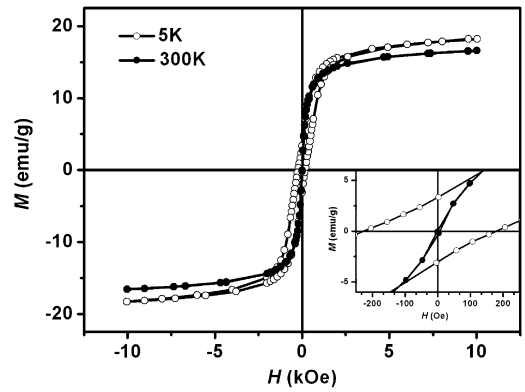

Figure 7. $M(H)$ hysteresis loops measured at $T = 5$ and 300 K for the 1D chains of hollow Fe_3O_4 spheres. The inset depicts the details of the hysteresis loop in the low-field region.

substrate in acidic solution and ball milling Fe nanoparticles in aqueous solution.[33,34] Therefore, the partial pressure of oxygen is considered as an important role in the formation of 1D chainlike Fe_3O_4 hollow spheres. However, the accurate relationship between oxygen partial pressure and diffusion rate in the iron oxide layer has not yet been revealed.

Magnetic properties of the chainlike Fe_3O_4 hollow nanospheres were characterized in a powder collection by using a SQUID magnetometer (Quantum Design), recording $M-T$ curves and $M-H$ loops. As shown in Figure 6, the $M_{ZFC}(T)$ and $M_{FC}(T)$ curves in a log Y scale reveal the inflections at 65 K, as pointed by the double-headed arrow, indicating the Verwey transition. The Verwey transition marks a structural transition of magnetite from a high-temperature cubic phase to a low-temperature monoclinic one. The transition temperature T_V obviously reduced from its bulk value of ~120 K, which has also been observed in the case of 50−200 nm Fe_3O_4 nanoparticles.[35,36] The inset shows that a broad maximum appears at about $T = 300$ K in the $M_{ZFC}(T)$ curve, which is a signature of the blocking temperature T_B. The broad maximum around T_B and the slight separation between the $M_{ZFC}(T)$ and $M_{FC}(T)$ curves above T_B are attributed to the small size of the nanocrystallites composing the hollow shell. Combining the nanocrystallite size obtained from TEM and XRD results, the effective anisotropy barrier is estimated as $2.1-5.8 \times 10^4$ J/m^3 according to the equation $K_{eff}V = 25k_BT_B$. At $T > T_V$, the magnetocrystalline anisotropy is expected to be cubic with the first anisotropy constant $K_1 < 0$. Thus, $|K_1|$ is determined as $2.5-7.0 \times 10^5$ J/m^3 by the relation $K_{eff} = |K_1|/12$.[37] This value is larger than the bulk one, $|K_1^{bulk}| = 1.1-1.3 \times 10^4$ J/m^3 at room temperature, by 1 order of magnitude.[38] The mechanism of the much enhanced anisotropy is unspecific. Though the interparticle dipolar interaction might have a significant effect on the enhanced anisotropy,[35,39] the shape anisotropy of the quasi-2D shell of the chainlike hollow nanospheres is the probable one that explains the effect in the best way.[40−42]

Figure 7 shows the field dependent $M(H)$ curves at $T = 5$ and 300 K. The saturation magnetization determined in the high-field region at 300 K is 16.6 emu/g, which accounts for only 18% of the bulk value, ~94 emu/g. Similar phenomena have been observed with nanosized Ni hollow spheres ~24% and hollow Co chains ~23% of the corresponding bulk value.[8,43] The reduction of the saturation magnetization is probably attributed to the existence of noncollinear spins or defects on the surface, as well as the nonmagnetic surfactant layers.[44] The thermogravimetry analysis (TGA) curves of the as-obtained samples show a weight loss of nonmagnetic residues of about 35% (see Supporting Information Figure S3). The coercivities are determined as 200 Oe at $T = 5$ K and 2 Oe at $T = 300$ K, which agree well with the changing separated gap between $M_{ZFC}(T)$ and $M_{FC}(T)$ curves.

Conclusion

In conclusion, 1D chainlike hollow magnetic Fe_3O_4 spheres have been successfully prepared by *in situ* oxidizing preassembled Fe nanoparticles in aqueous solution at room temperature. An iron oxide layer formed on the surface of 1D Fe nanoparticle arrays, thus fixing and stabilizing the linear chainlike structures and making it more stable without any other cross-link reagents. These hollow nanostructures are supposed to form based on the nanoscale Kirkendall effect. Besides the aqueous microenvironment, the partial pressure of oxygen is of great importance in the formation of 1D chainlike Fe_3O_4 hollow nanostructures. This synthetic strategy may extend to other transition metal oxide systems with 1D hollow structure. In addition, 1D chainlike hollow structures of Fe_3O_4 are also expected to have potential applications in catalysis, drug delivery, and other magnetic related applications.

Acknowledgment. We acknowledge NSFC (Nos. 20671004 and 20821091), MOST of China (No. 2009CB939902), MOE of China (No. 707002), and Delta Electronics Inc.

Supporting Information Available: Additional experimental details, controlled experiments, UV−vis absorption spectra, and TGA data. This material is available free of charge via the Internet at http://pubs.acs.org.

References and Notes

(1) Yin, Y. D.; Rioux, R. M.; Erdonmez, C. K.; Hughes, S.; Somorjai, G. A.; Alivisatos, A. P. *Science* **2004**, *304*, 711.
(2) Kim, S. W.; Kim, M.; Lee, W. Y.; Hyeon, T. *J. Am. Chem. Soc.* **2002**, *124*, 7642.
(3) Sun, Y. G.; Mayers, B.; Xia, Y. N. *Adv. Mater.* **2003**, *15*, 641.
(4) Hu, Y.; Jiang, X. Q.; Ding, Y.; Chen, Q.; Yang, C. Z. *Adv. Mater.* **2004**, *16*, 933.
(5) Li, B. X.; Xie, Y.; Jing, M.; Rong, G. X.; Tang, Y. C.; Zhang, G. Z. *Langmuir* **2006**, *22*, 9380.
(6) Wu, W.; DeCoster, M. A.; Daniel, B. M.; Chen, J. F.; Yu, M. H.; Cruntu, D.; O'Connor, C. J.; Zhou, W. L. *J. Appl. Phys.* **2006**, *99*, 08H104.
(7) Liu, Q.; Liu, H. J.; Han, M.; Zhu, J. M.; Liang, Y. Y.; Xu, Z.; Song, Y. *Adv. Mater.* **2005**, *17*, 1995.

(8) Guo, L.; Liang, F.; Wen, X. G.; Yang, S. H.; He, L.; Zheng, W. Z.; Chen, C. P.; Zhong, Q. P. *Adv. Funct. Mater.* **2007**, *17*, 425.
(9) Vasquez, Y.; Sra, A. K.; Schaak, R. E. *J. Am. Chem. Soc.* **2005**, *127*, 12504.
(10) Zhai, J. F.; Huang, M. H.; Zhai, Y. M.; Dong, S. J. *J. Mater. Chem.* **2008**, *18*, 923.
(11) Cheng, F. Y.; Ma, H.; Li, Y. M.; Chen, J. *Inorg. Chem.* **2007**, *46*, 788.
(12) Huang, J.; He, L.; Leng, Y. H.; Zhang, W.; Li, X. G.; Chen, C. P.; Liu, Y. *Nanotechnology* **2007**, *18*, 415603.
(13) Peng, S.; Sun, S. H. *Angew. Chem., Int. Ed.* **2007**, *46*, 4155.
(14) Li, X. H.; Zhang, D. H.; Chen, J. S. *J. Am. Chem. Soc.* **2006**, *128*, 8382.
(15) Yu, D. B.; Sun, X. Q.; Zou, J. W.; Wang, Z. R.; Wang, F.; Tang, K. *J. Phys. Chem. B* **2006**, *110*, 21667.
(16) Chen, X. Y.; Zhang, Z. J.; Li, X. X.; Shi, C. W. *Chem. Phys. Lett.* **2006**, *422*, 284.
(17) Jia, B. P.; Gao, L. *J. Phys. Chem. C* **2008**, *112*, 666.
(18) Latham, A. H.; Wilson, M. J.; Schiffer, P.; Williams, M. E. *J. Am. Chem. Soc.* **2006**, *128*, 12632.
(19) Butter, K.; Bomans, P. H.; Frederik, P. M.; Vroege, G. J.; Philipse, A. P. *Nat. Mater.* **2003**, *2*, 88.
(20) Furst, E. M.; Suzuki, C. M.; Fermigier, M.; Gast, A. P. *Langmuir* **1998**, *14*, 7334.
(21) Nakata, K.; Hu, Y.; Uzun, O.; Bakr, O.; Stellacci, F. *Adv. Mater.* **2008**, *20*, 4284.
(22) Hegde, M. S.; Larcher, D.; DuPont, L.; Beaudoin, B.; Tekaia-Elhsissen, K.; Tarascon, J. M. *Solid State Ionics* **1996**, *93*, 33.
(23) Tong, G. X.; Guan, J. G.; Xiao, Z. D.; Mou, F. Z.; Wang, W.; Yan, G. Q. *Chem. Mater.* **2008**, *20*, 3535.
(24) Wang, N.; Cao, X.; Kong, D. S.; Chen, W. M.; Guo, L.; Chen, C. P. *J. Phys. Chem. C* **2008**, *112*, 6613.
(25) Cabot, A.; Puntes, V. F.; Shevchenko, E.; Yin, Y. D.; Balcells, L.; Marcus, M. A.; Hughes, S. M.; Alivisatos, A. P. *J. Am. Chem. Soc.* **2007**, *129*, 10358.
(26) Zeng, J.; Huang, J. L.; Lu, W.; Wang, X. P.; Wang, B.; Zhang, S. Y.; Hou, J. G. *Adv. Mater.* **2007**, *19*, 2172.
(27) Gao, J. H.; Zhang, X. B.; Zhang, X.; Xu, B. *Angew. Chem., Int. Ed.* **2006**, *45*, 1220.
(28) Yin, Y. D.; Erdonmez, C. K.; Cabot, A.; Hughes, S.; Alivisatos, A. P. *Adv. Funct. Mater.* **2006**, *16*, 1389.
(29) Sarathy, V.; Tratnyek, P. G.; Nurmi, J. T.; Baer, D. R.; Amonette, J. E.; Chun, C. L.; Penn, R. L.; Reardon, E. J. *J. Phys. Chem. C* **2008**, *112*, 2286.
(30) Leibbrandt, G. W.; Hoogers, G.; Habraken, F. H. P. M. *Phys. Rev. Lett.* **1992**, *68*, 1947.
(31) Wang, C. M.; Baer, D. R.; Thomas, L. E.; Amonette, J. E.; Antony, J. J.; Qiang, Y.; Duscher, G. *J. Appl. Phys.* **2005**, *98*, 094308.
(32) Linderoth, S.; Morup, S.; Bentzon, M. D. *J. Mater. Sci.* **1995**, *30*, 3142.
(33) Chin, K. C.; Chong, G. L.; Poh, C. K.; Van, L. H.; Sow, C. H.; Lin, J. Y.; Wee, A. T. S. *J. Phys. Chem. C* **2007**, *111*, 9136.
(34) Janot, R.; Guerard, D. *J. Alloys Compd.* **2002**, *333*, 302.
(35) Goya, G. F.; Berquó, T. S.; Fonseca, F. C.; Morales, M. P. *J. Appl. Phys.* **2003**, *94*, 3520.
(36) Song, P. Y.; Wang, J. F.; Chen, C. P.; Deng, H.; Li, Y. D. *J. Appl. Phys.* **2006**, *100*, 044314.
(37) García-Otero, J.; Porto, M.; Rivas, J.; Bunde, A. *J. Appl. Phys.* **1999**, *85*, 2287.
(38) Cullity, B. D. *Introduction to Magnetic Materials*; Addison-Wesley: Reading, MA, 1972; p 234.
(39) Kong, D. S.; Chen, C. P.; He, L. *J. Appl. Phys.* **2008**, *103*, 114312.
(40) O'Handley, R. C. *Modern Magnetic Materials*; John Wiley & Sons: New York, 2000; p 39.
(41) He, L.; Zheng, W. Z.; Zhou, W.; Du, H. L.; Chen, C. P.; Guo, L. *J. Phys.: Condens. Matter* **2007**, *19*, 036216.
(42) Paulus, P. M.; Luis, F.; Kroll, M.; Schmid, G.; de Jongh, L. J. *J. Magn. Magn. Mater.* **2001**, *224*, 180.
(43) Li, Q.; Liu, H.; Han, M.; Zhu, J.; Liang, Y.; Xu, Z.; Song, Y. *Adv. Mater.* **2005**, *17*, 1995.
(44) Coey, J. M. D. *Phys. Rev. Lett.* **1971**, *27*, 1140.

JP810662J